

Summary of the Electroweak and Beyond the Standard Model Working Group

Christopher Hays¹, Michael Krämer², David M. South³, and Alexander Filip Żarnecki⁴

1- University of Oxford, Department of Physics
Oxford OX1 3RH, United Kingdom

2- Institute for Theoretical Physics, RWTH Aachen University
D-52056 Aachen, Germany

3- Technische Universität Dortmund - Experimentelle Physik V
D-44221 Dortmund, Germany

4- Institute of Experimental Physics, University of Warsaw
Hoża 69, 00-681 Warszawa, Poland

A wide array of deep-inelastic-scattering and hadron collider experiments have tested the predictions of the electroweak theory and measured its parameters, while also searching for new particles and processes. We summarise recent measurements and searches that probe the Standard Model to unprecedented precision.

1 Introduction

The production and study of particles through deep inelastic scattering is one of the main tools in high energy physics and has led to a comprehensive understanding of the fundamental particles and interactions up to the electroweak energy scale. Successful running of the HERA ep collider, $\sqrt{s} = 319$ GeV, has recently come to an end, and selected results are already available from the complete 1 fb^{-1} data set. The Tevatron continues to collide protons and antiprotons at $\sqrt{s} = 1.96$ TeV, with new analyses based on up to 3 fb^{-1} of data. Later this year the LHC will ramp up proton beams to $\sqrt{s} = 10$ TeV, to be followed next year by $\sqrt{s} = 14$ TeV pp collisions. In addition, data from the completed NuTeV fixed-target incident-neutrino experiment have been further analysed to test several hypotheses for the source of the long-standing $\sin^2 \theta_W$ discrepancy.

2 Electroweak Measurements

The Lagrangian describing the electroweak $SU(2)_L \times U(1)_Y$ symmetry, before symmetry breaking, is:

$$\mathcal{L}_{\text{EW}} = \mathcal{L}_{\text{g}} + \mathcal{L}_{\text{f}} + \mathcal{L}_{\text{h}} + \mathcal{L}_{\text{y}}.$$

The four components are the gauge term (\mathcal{L}_{g}), the fermion term (\mathcal{L}_{f}), the Higgs term (\mathcal{L}_{h}), and the Yukawa coupling term (\mathcal{L}_{y}). After the symmetry breaking via the Higgs mechanism, the Lagrangian describing the masses and interactions of the physical particles can be written as:

$$\mathcal{L}_{\text{EW}} = \mathcal{L}_{\text{K}} + \mathcal{L}_{\text{NC}} + \mathcal{L}_{\text{CC}} + \mathcal{L}_{\text{H}} + \mathcal{L}_{\text{HV}} + \mathcal{L}_{\text{WVW}} + \mathcal{L}_{\text{WVWV}} + \mathcal{L}_{\text{Y}}.$$

The Lagrangian now includes a kinetic term (\mathcal{L}_{K}), a neutral current term (\mathcal{L}_{NC}), a charged current term (\mathcal{L}_{CC}), a Higgs self-coupling term (\mathcal{L}_{H}), a Higgs-gauge interaction term (\mathcal{L}_{HV}), a trilinear gauge interaction term (\mathcal{L}_{WVW}), a quartic gauge interaction term ($\mathcal{L}_{\text{WVWV}}$), and a Yukawa term (\mathcal{L}_{Y}). Only an electromagnetic $U(1)_{\text{EM}}$ symmetry survives.

Ongoing and completed experiments continue to test many of the terms in the broken electroweak Lagrangian, and the LHC experiments are making final sensitivity estimates before first data.

2.1 Trilinear Gauge Couplings

The Lagrangian for trilinear gauge couplings is:

$$\begin{aligned} \mathcal{L}_{WWV} = & -ig[(W_{\mu\nu}W^\mu - W^\mu W_{\mu\nu})(A^\nu \sin\theta_W - Z^\nu \cos\theta_W) \\ & + W_\nu W_\mu (A^{\mu\nu} \sin\theta_W - Z^{\mu\nu} \cos\theta_W)]. \end{aligned} \quad (1)$$

Recent Tevatron measurements of $W\gamma$, WZ , $Z\gamma$ and ZZ production have probed the trilinear gauge vertices of the electroweak theory. $W\gamma$ production at the Tevatron occurs predominantly through separate W and γ radiation from quarks in the t - and u -channels, with a smaller contribution from the s -channel triple-gauge vertex. A study of this vertex can be made through its interference with the other channels. The interference produces a dip in the $Q_l \times \Delta y$ distribution, where Q_l is the charge of the lepton from the W boson decay and Δy is the rapidity difference between the lepton and the photon. This dip is known as a *radiation amplitude zero* and appears at $Q_l \times \Delta\eta \approx -1/3$, where the pseudorapidity η equals the rapidity in the massless limit.

$D\bar{O}$ has probed the $l^\pm\nu\gamma$ final state for evidence of the s -channel interference [1]. A dip is observed consistent with the predicted radiation amplitude zero, as shown in Figure 1, and has a 2.6σ significance relative to a monotonic curve. $D\bar{O}$ has also searched for anomalous triple-gauge couplings that modify the $W_\nu W_\mu A^{\mu\nu}$ term in Equation 1 by a scale factor $\kappa_\gamma/(1 + \hat{s}/\Lambda^2)^2$, and that introduce a new term $ig\lambda_\gamma/[(1 + \hat{s}/\Lambda^2)^2 M_W^2] W_{\lambda\mu} W_\nu^\mu A^{\nu\lambda}$, for a cut-off energy scale $\Lambda = 2$ TeV. These terms enhance the production cross section for high-momentum photons, and since no enhancement is observed, limits of $0.49 < \kappa_\gamma < 1.51$ and $-0.12 < \lambda_\gamma < 0.13$ are placed on these couplings.

The Tevatron is currently the only place to separately study the WWZ and $WW\gamma$ vertices. As with $W\gamma$ production, WZ production at the Tevatron includes both an s -channel diagram with a triple-gauge vertex and t - and u -channel diagrams where the bosons are radiated off the quarks. Destructive interference is large in WZ production, and the WWZ vertex significantly reduces the cross section, as shown in Figure 2. CDF has observed WZ production at the 6σ level [2] in the $l\nu l'l'$ final state, measuring a cross section

$$\sigma_{WZ} = 4.4_{-1.0}^{+1.3} \text{ stat} \pm 0.4_{\text{sys+lum}} \text{ pb}$$

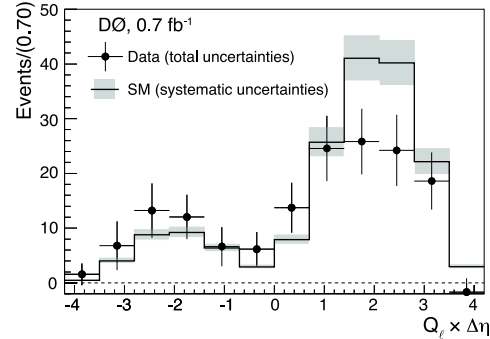


Figure 1: The $D\bar{O}$ charge-signed pseudorapidity difference between the charged lepton and the photon. The dip at $Q_l \times \Delta\eta \approx -1/3$ is consistent with the interference due to the trilinear $WW\gamma$ coupling and has a significance of 2.6σ .

that is consistent with the next-to-leading order (NLO) prediction of $\sigma_{WZ} = 3.7 \pm 0.3$ pb. Both CDF and DØ set limits (Table 1) on the anomalous coupling parameters λ_Z and $\Delta\kappa_Z = \kappa_Z - 1$, which are the analogues to the $WW\gamma$ vertex parameters. Limits are also set on $\Delta g_1^Z = g_1^Z - 1$, where g_1^Z is a scale factor for the $(W_{\mu\nu}W^\mu - W^\mu W_{\mu\nu})$ term.

The Standard Model (SM) does not have trilinear gauge vertices involving only neutral particles. The Tevatron experiments test this prediction by studying $Z\gamma$ and ZZ production. CDF and DØ select $Z\gamma$ events in the $l\gamma$ final state, requiring $E_T^\gamma > 7$ GeV and $\Delta R(l, \gamma) > 0.7$. Using 778 and 968 candidates respectively, CDF and DØ measure $Z\gamma$ production cross sections of

$$\begin{aligned}\sigma_{Z\gamma}^{\text{CDF}} &= 4.6 \pm 0.4_{\text{stat+sys}} \pm 0.3_{\text{lum}} \text{ pb} \\ \sigma_{Z\gamma}^{\text{DØ}} &= 5.0 \pm 0.3_{\text{stat+sys}} \pm 0.3_{\text{lum}} \text{ pb},\end{aligned}$$

consistent with the NLO SM prediction of $\sigma_{Z\gamma} = 4.5 \pm 0.4$ pb. Limits are set on anomalous couplings using the consistency of data and prediction at high photon momentum.

The rare process of ZZ production is now beginning to appear at the Tevatron. CDF has three candidate events in the four-lepton final state [3], and with a background of only 0.1 ± 0.1 this constitutes a 4.2σ evidence. Combining with 276 candidate events in the $ll\nu\nu$ channel, where a likelihood discriminant is used to separate the 14 expected ZZ events, gives a total significance of 4.4σ . The measured cross section of $\sigma_{ZZ} = 1.4^{+0.7}_{-0.6}$ pb is consistent with the NLO prediction of $\sigma_{ZZ} = 1.4 \pm 0.1$ pb. Recently DØ has claimed a 5.7σ observation of ZZ production [4].

2.2 Charged and Neutral Currents

The charged and neutral current contributions to the SM Lagrangian can be expressed as:

$$\begin{aligned}\mathcal{L}_{\text{CC}} &= -\frac{g}{\sqrt{2}} \left[\bar{u}_i \gamma^\mu \frac{1-\gamma^5}{2} M_{ij}^{\text{CKM}} d_j + \bar{\nu}_i \gamma^\mu \frac{1-\gamma^5}{2} e_i \right] W_\mu^+ + \text{h.c.} \quad \text{and} \\ \mathcal{L}_{\text{NC}} &= e J_\mu^{\text{em}} A^\mu + \frac{g}{\cos\theta_W} (J_\mu^3 - \sin\theta_W J_\mu^{\text{em}}) Z^\mu.\end{aligned}$$

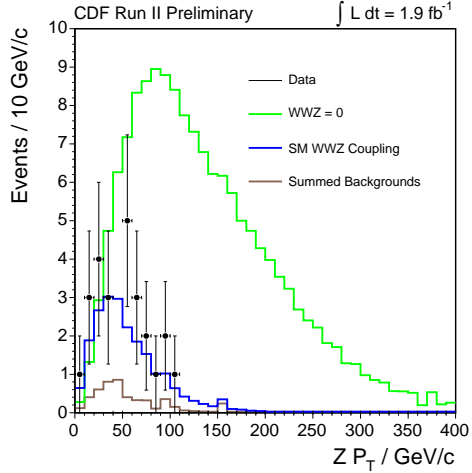


Figure 2: The P_T of the reconstructed Z boson in WZ production at CDF. The interference between diagrams with and without the WWZ vertex significantly suppresses the cross section, and the data are consistent with this suppression.

Coupling	CDF	DØ
λ_Z	(-0.13, 0.14)	(-0.17, 0.21)
Δg_1^Z	(-0.13, 0.23)	(-0.14, 0.34)
$\Delta\kappa_Z$	(-0.76, 1.18)	(-0.12, 0.29)*

Table 1: Limits on anomalous WWZ couplings for a cut-off scale of $\Lambda = 2$ TeV. *DØ limits on $\Delta\kappa_Z$ are for the case $\Delta\kappa_Z = \Delta g_1^Z$.

Table 1: Limits on anomalous WWZ couplings for a cut-off scale of $\Lambda = 2$ TeV. *DØ limits on $\Delta\kappa_Z$ are for the case $\Delta\kappa_Z = \Delta g_1^Z$.

The electromagnetic current J_μ^{em} is vector-like (V), coupling equally to left- and right-handed helicity states. The weak current J_μ^3 is of a vector-minus-axial ($V - A$) nature, coupling only to left-handed helicity states. The CKM matrix M_{ij}^{CKM} determines the mixing between mass and weak eigenstates of the quarks.

The electroweak couplings have no dependence on fermion generation. This property has been tested with a measurement of the charged kaon decay rate ratio $R_K = \Gamma(K^\pm \rightarrow e^\pm \nu) / \Gamma(K^\pm \rightarrow \mu^\pm \nu)$ at the NA48 and NA62 experiments at CERN. The 2004 measurement of $R_K = 2.455 \pm 0.045_{\text{stat}} \pm 0.041_{\text{sys}} \times 10^{-5}$ is consistent with the SM prediction of $R_K = 2.477 \times 10^{-5}$ and has a systematic uncertainty dominated by the background prediction. New methods to constrain the background using data are in progress, promising a significant reduction in the uncertainty of this measurement. A recent review of precision SM tests with kaons can be found in [5].

Polarised electron beams in the ep collisions at HERA allow a test of the $V - A$ structure of the weak coupling, represented by the $(1 - \gamma^5)/2$ factor in the Lagrangian. The cross section of the charged current process $ep \rightarrow \nu X$ is a linear function of lepton polarisation, going to zero for right-handed electrons and left-handed positrons. The ZEUS Collaboration has measured this cross section for polarisations of -0.27 and 0.33 for e^-p collisions and -0.36 and 0.32 for e^+p collisions, where the polarisation P_e equals one for right-handed lepton beams [6]. Combining with unpolarised measurements, the observed cross section dependence on polarisation is consistent with the SM, as shown in Figure 3.

Another test of the $V - A$ nature of charged current interactions occurs through a measurement of the W boson helicity in top quark decays. The helicity has a longitudinal component due to the W boson mass and a left-handed component due to the W boson coupling. CDF uses several techniques to measure the helicity in $t\bar{t} \rightarrow WbWb \rightarrow l\nu bqqb$ events [7]. One method uses the relative angle (θ^*) between the top quark and final-state charged lepton in the W boson rest frame. The measured distribution of $\cos\theta^*$ is consistent with the SM prediction of 70% longitudinal helicity, as can be seen in Figure 4. The most

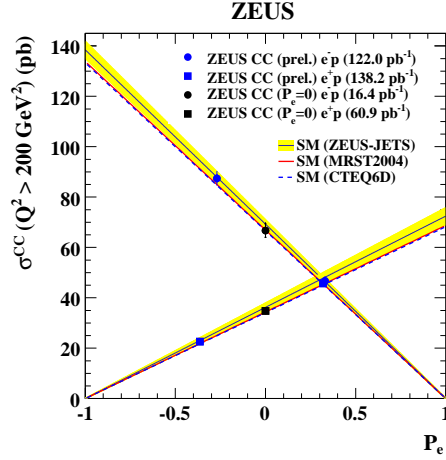


Figure 3: The measured and theoretical charged current cross section in $e^\pm p$ collisions, as a function of lepton polarisation. The ZEUS measurements are consistent with the $V - A$ structure of the weak interaction.

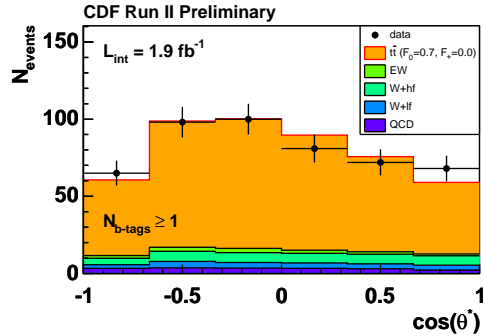


Figure 4: The $\cos\theta^*$ distribution in $t\bar{t} \rightarrow WbWb \rightarrow l\nu bqqb$ events, where θ^* is the angle between the top quark and the charged lepton in the W boson rest frame.

precise CDF and DØ measurements of the longitudinal helicity of the W boson in top decays are $0.64 \pm 0.08_{\text{stat}} \pm 0.07_{\text{sys}}$ and $0.62 \pm 0.09_{\text{stat}} \pm 0.05_{\text{sys}}$, respectively.

The CKM matrix elements M_{ij}^{CKM} arise from off-diagonal Higgs-quark Yukawa couplings in generation space before symmetry breaking. These couplings are not predicted by the SM and must be measured. The element V_{tb} can be determined with a measurement of single top production at the Tevatron, since the cross section of the process $p\bar{p} \rightarrow W \rightarrow t\bar{b}$ includes a factor of $|V_{tb}|^2$. Both CDF and DØ [8] have obtained evidence for single top production, with measured cross sections and $|V_{tb}|$ limits of

$$\begin{aligned}\sigma_{tb}^{\text{CDF}} &= 2.2 \pm 0.7 \text{ pb } (|V_{tb}| > 0.66) \\ \sigma_{tb}^{\text{DØ}} &= 4.7 \pm 1.3 \text{ pb } (|V_{tb}| > 0.68).\end{aligned}$$

Experiments at the LHC will also measure single top production in the process $pp \rightarrow W \rightarrow t\bar{b}$, and expect to constrain $|V_{tb}|$ to 5% with 10 fb^{-1} of data.

The fermion vector (v_f) and axial (a_f) couplings to the neutral current are determined by the relative $\text{SU}(2)_L$ and $\text{U}(1)_Y$ couplings g and g' respectively. These couplings were probed in electron-quark interactions at HERA, through neutral current photon and Z^0 exchange in the t - and u -channels. The experiments extract the vector (v_q) and axial (a_q) quark couplings from a global fit to the neutral current and charged current inclusive and jet cross sections. The inclusion of charged current data constrains the parton distribution functions, which are needed to extract the couplings. Figure 5 shows the latest fits for v_u , a_u , v_d , and a_d from ZEUS [9] and H1 [10] global fits.

The weak mixing angle is defined in terms of the $\text{SU}(2)_L$ and $\text{U}(1)_Y$ couplings using the parameterisation $\tan \theta_W = g'/g$. By measuring neutral current and charged current cross sections in neutrino-nucleon and antineutrino-nucleon scattering, $\sin^2 \theta_W$ can be extracted from the Paschos-Wolfenstein relation:

$$R = \frac{\sigma_{\text{NC}}^\nu - \sigma_{\text{NC}}^{\bar{\nu}}}{\sigma_{\text{CC}}^\nu - \sigma_{\text{CC}}^{\bar{\nu}}} = \rho^2 \left(\frac{1}{2} - \sin^2 \theta_W \right).$$

The NuTeV experiment measured $\sin^2 \theta_W = 0.2277 \pm 0.0013_{\text{stat}} \pm 0.0009_{\text{sys}}$, which is nearly 3σ above the latest fit to electroweak data ($\sin^2 \theta_W = 0.2231 \pm 0.0003$). The discrepancy is

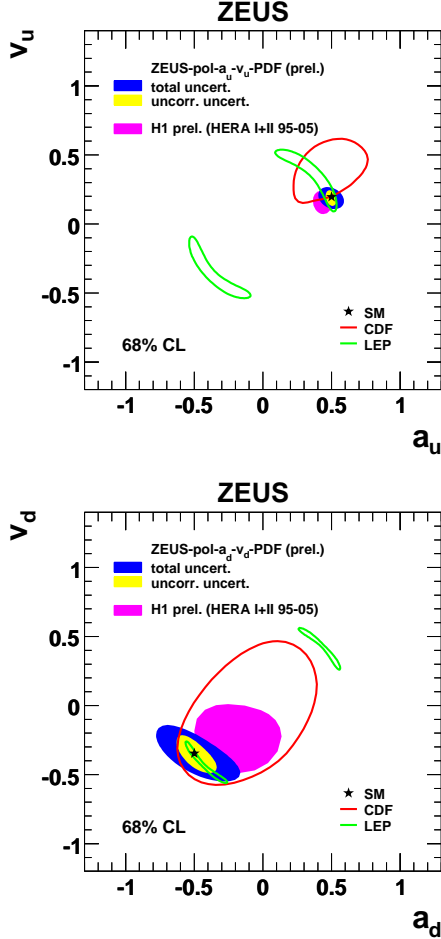


Figure 5: The vector and axial neutral current couplings for up (top) and down (bottom) quarks from ZEUS, H1, CDF, and LEP.

dominantly in the neutrino cross sections, where the ratio of neutral current to charged current cross sections (R^ν) is nearly 3σ below expectation ($\Delta R^\nu = -0.0034 \pm 0.0013$). NuTeV has updated R^ν , and the equivalent ratio for antineutrino–nucleon scattering ($R^{\bar{\nu}}$), factoring in several new results: a fit to its charm–decay data for a possible strange–antistrange asymmetry in the nucleon; the latest $K^+ \rightarrow \pi^0 e^+ \nu$ (K_{e3}^+) branching ratio; and an improved d/u PDF uncertainty estimate. The effects respectively decrease, increase, and slightly increase the discrepancy in R^ν relative to the prediction, giving an updated deviation of $\Delta R^\nu = -0.0038 \pm 0.0013$ [11]. Further updates are expected to incorporate QED corrections to the PDFs and charm-mass effects.

2.3 Yukawa Couplings (Top Mass)

The Yukawa Higgs–fermion couplings determine the masses of all the fermions:

$$\mathcal{L}_Y = -i \sum_f \frac{g m_f}{2m_W} \bar{f} f H.$$

Of particular interest is the top quark Yukawa coupling, which is much larger than all other Yukawa couplings and has a natural value close to one. The large top mass results in significant radiative corrections to the gauge boson masses, and must be precisely known to use radiative corrections to constrain the Higgs mass.

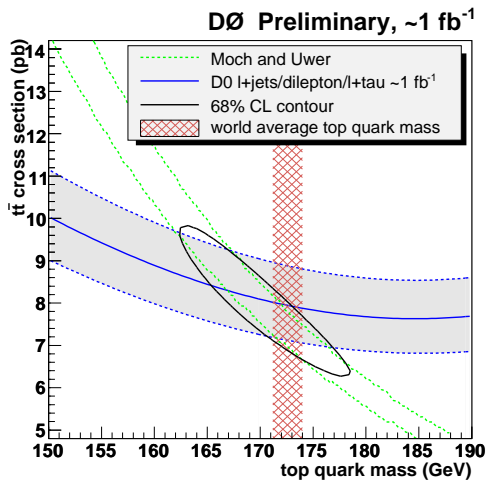


Figure 6: The predicted and measured $t\bar{t}$ cross section as a function of top quark mass. DØ uses the mass dependence of the cross section to extract $m_t = 169.6^{+5.4}_{-5.5}$ GeV.

Of particular interest is the top quark Yukawa coupling, which is much larger than all other Yukawa couplings and has a natural value close to one. The large top mass results in significant radiative corrections to the gauge boson masses, and must be precisely known to use radiative corrections to constrain the Higgs mass.

The top quark has only been observed at the Tevatron, and both CDF and DØ continue to update their measurements of the top mass. The measurements predominantly rely on reconstructing the top quarks in $t\bar{t}$ decays to $l\nu l\nu b\bar{b}$ (dilepton + jets), $l\nu q\bar{q}b\bar{b}$ (lepton + jets), and $q\bar{q}q\bar{q}b\bar{b}$ (all-hadronic). The most precise result is in the lepton + jets final state, where the light-flavor quarks are constrained to the W boson mass, reducing the jet energy scale uncertainty. The latest combined CDF and DØ result gives $m_t = 172.4 \pm 1.2$ GeV [12]. The LHC experiments expect to achieve $\delta m_t = 1$ GeV with their first fb^{-1} of data.

An independent determination of the mass can be obtained through the $t\bar{t}$ cross section measurement, since the cross section has a significantly decreasing slope as a function of mass. DØ has used its precise measurement of $\sigma_{t\bar{t}} = 7.62 \pm 0.85$ pb to extract $m_t = 170 \pm 7$ GeV [13]. Recently, DØ has compared the result to two new theoretical calculations, one based on NLO+NLL soft–gluon summation [14] and the other including all soft–gluon induced NNLL terms contributing at NNLO [15]. DØ has also combined cross section measurements in the lepton + jets, dilepton + jets, and lepton + tau

+ jets channels, obtaining its most precise mass determination based on the cross section, $m_t = 169.6_{-5.5}^{+5.4}$ GeV, as illustrated in Figure 6.

2.4 Kinetic Terms (Higgs Boson)

Of the terms in the kinetic Lagrangian,

$$\begin{aligned} \mathcal{L}_K = & \sum_f \bar{f}(i\cancel{\partial} - m_f)f - \frac{1}{4}A_{\mu\nu}A^{\mu\nu} - \frac{1}{2}W_{\mu\nu}^+W^{-\mu\nu} + m_W^2W_\mu^+W^{-\mu} - \\ & \frac{1}{4}Z_{\mu\nu}Z^{\mu\nu} + \frac{1}{2}m_Z^2Z_\mu Z^\mu + \frac{1}{2}(\partial^\mu H)(\partial_\mu H) - \frac{1}{2}m_H^2H^2, \end{aligned}$$

only those associated with the Higgs boson have yet to be tested. Direct searches from LEP have constrained the Higgs mass m_H to be greater than 114 GeV at 95% confidence level (C.L.), and an indirect constraint from a global fit to electroweak data requires $m_H < 160$ GeV with a best fit of $m_H = 87_{-27}^{+36}$ GeV (using $m_t = 172.6 \pm 1.4$ GeV). The LHC experiments expect to measure m_W to a precision of ≈ 5 MeV. Combined with the anticipated precision in the top mass measurement of ≈ 1 GeV, the indirect constraint on the Higgs mass should reach a precision of about 15 GeV at the LHC.

In the Higgs mass range allowed by the electroweak precision data, the Tevatron has the potential to exclude or obtain evidence for the SM Higgs with a complete data set of ≈ 7 fb $^{-1}$. In the low-mass region ($m_H \lesssim 130$ GeV), where the Higgs dominantly decays to $b\bar{b}$, the searches focus on WH and ZH production. A recent gain in sensitivity has come from including the $H \rightarrow \tau\tau$ decay, with a branching ratio about 10% that of $b\bar{b}$ and with lower background. In the high-mass region ($m_H \gtrsim 130$ GeV), $H \rightarrow WW$ is the dominant decay mode, and sensitivity comes primarily from a search for $gg \rightarrow H \rightarrow WW \rightarrow l\nu l'\nu'$. A recent improvement in all decay channels has come from including the vector-boson-fusion production mechanism [16]. The CDF and DØ experiments have announced the exclusion of a Higgs with $m_h = 170$ GeV, as shown in Figure 7. With the data continuing to be collected, the exclusion region will expand quickly and could turn into a claim for evidence of Higgs production.

While the low-mass region is challenging for the LHC experiments, an updated sensitivity study shows that discovery can be achieved with just 5 fb $^{-1}$ for every Higgs mass by combining CMS and ATLAS searches.

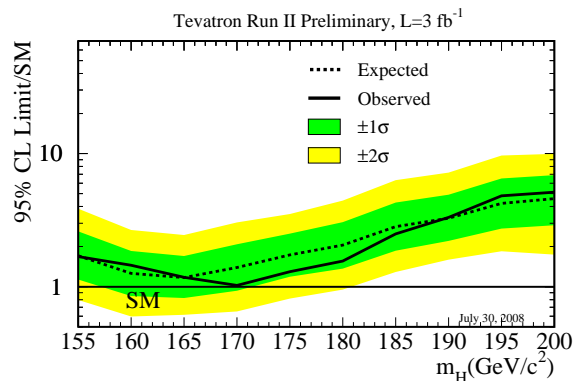


Figure 7: The ratio of excluded to SM cross section as a function of Higgs boson mass. A Higgs boson with mass equal to 170 GeV is excluded.

3 Beyond the Standard Model Searches

3.1 Searches for Rare Processes at High Transverse Momentum

3.1.1 General Searches for New Physics

The H1 Collaboration has performed a generic search for deviations from the SM at large values of transverse momentum $P_T > 20$ GeV in the full H1 data set of 0.5 fb^{-1} [17]. All high P_T final-state configurations involving electrons (e), muons (μ), jets (j), photons (γ) or neutrinos (ν) are systematically investigated in exclusive classes, formed according to the number and types of objects detected in the final state (e.g. e - j , μ - j - ν , j - j - j - j). Event yields are shown in Figure 8 for the H1 HERA II e^+p data, where no significant deviation from the SM is observed in the phase space and event topologies covered by the analysis.

A similar global search for new physics based on a systematic search for discrepancies with respect to the SM has also been performed by CDF using 2 fb^{-1} of high P_T data, where 399 exclusive final states and almost 20000 kinematic distributions are searched [18]. Although a number of interesting effects are observed, the search reveals no indication of physics beyond the Standard Model.

3.1.2 Events with High- P_T Leptons

Measurements of final states with multiple high P_T electrons and muons are performed by H1 and ZEUS [19]. Within the SM the production of multi-lepton events in ep collisions mainly proceeds via photon-photon interactions. The observed event yields are in good agreement with SM expectations, although in the H1 analysis an excess of data events is observed at high masses in the e^+p data. A common phase space has been established in order to combine the results of the two experiments, using a total integrated luminosity of 0.94 fb^{-1} [20]. As an example, for multi-electron events the distribution of the scalar sum of all electron transverse momenta $\sum P_T$ is shown in Figure 9 (left) for 2 and 3 electron events in the e^+p data. For $\sum P_T > 100$ GeV a slight excess is present with 5 events observed in the data, compared to a SM expectation of 1.8 ± 0.2 . No such excess is seen in the e^-p data.

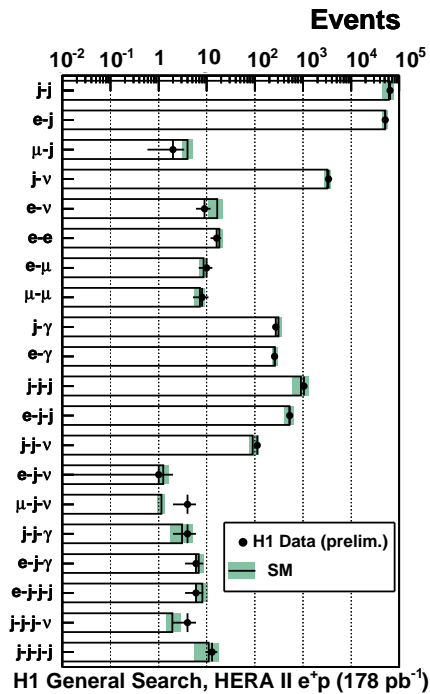


Figure 8: The data and SM expectation for all event classes with observed data events or a SM expectation greater than 1 event in the H1 general search analysis of the HERA II e^+p data. The error bands on the predictions include model uncertainties and experimental systematic errors added in quadrature.

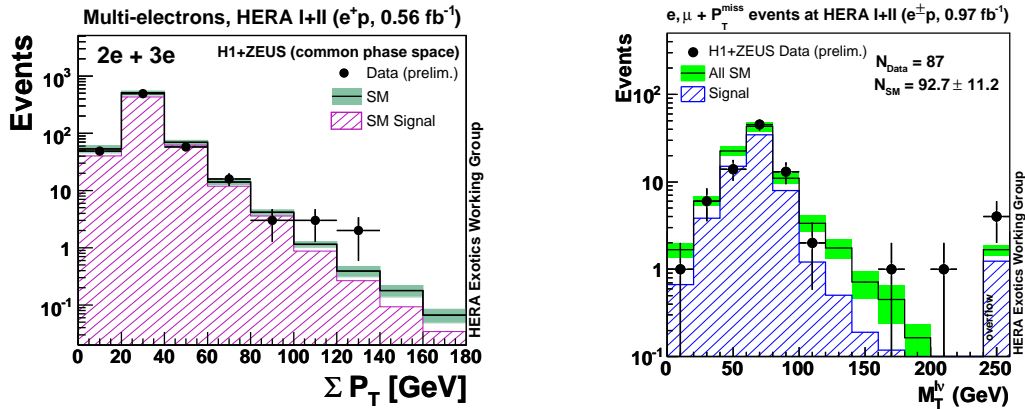


Figure 9: Left: The scalar sum of the electron transverse momenta for events with 2 or 3 electrons in the combined H1+ZEUS e^+p data. Right: The transverse mass $M_T^{l\nu}$ distribution for events with the isolated lepton and missing transverse momentum in the combined H1+ZEUS $e^\pm p$ data. The data (points) are compared to the SM expectation (open histogram). The signal component of the SM expectation (left: photon–photon interactions, right: W production) is given by the hatched histogram. N_{Data} is the total number of data events observed and N_{SM} is the total SM expectation. The total uncertainty on the SM expectation is given by the shaded band.

Searches for events containing isolated leptons (electrons, muons or tau leptons) in coincidence with large missing transverse momentum are also performed by the H1 and ZEUS Collaborations [21]. Such events occur at HERA within the SM via W production with subsequent leptonic decay, which has a cross section of order 1 pb. The full HERA data has been analysed by both H1 and ZEUS. The latest electron and muon results from H1 reveal no excess over the SM for the e^-p data. However, the previously observed excess over SM prediction persists in the e^+p data at large hadronic transverse momentum, $P_T^X > 25$ GeV, where 21 data events are observed compared to an expectation of 8.9 ± 1.5 . The electron and muon results from ZEUS show no excess over the SM prediction. Similarly, H1 observes good agreement with the SM in its search for events with isolated tau leptons and missing P_T . H1 and ZEUS have combined their data in the electron and muon channels, resulting in a data set with a total integrated luminosity of 0.97 fb^{-1} [22]. The distribution of the reconstructed transverse mass $M_T^{l\nu}$ of the H1 and ZEUS events in the complete $e^\pm p$ HERA data is shown in Figure 9 (right), where a clear Jacobian peak is observed, consistent with the expectation from SM W production.

Events containing isolated leptons and large missing transverse momentum would be produced at HERA in several models of physics beyond the SM such as single top production via flavour–changing neutral current (FCNC) [23]. In particular, this process would produce events with large values of P_T^X , whereas SM W production is expected to predominantly produce events with small P_T^X . The H1 events are interpreted in this model, and using a maximum likelihood method an upper limit on the anomalous top production cross section of $\sigma_{ep \rightarrow etX} < 0.16$ pb is established at 95% C.L., corresponding to a limit on the anomalous coupling $\kappa_{tu\gamma} < 0.14$, which is currently the world’s most stringent limit. The

CDF Collaboration performs a search for the FCNC decay of the top quark $t \rightarrow Zq$ using 1.9 fb^{-1} of Tevatron Run II data [24]. $Z + \geq 4$ jets candidate events are used, both with and without a secondary vertex b -tag, and the background is rejected using kinematic constraints present in FCNC events. In the absence of a signal an upper limit on the branching fraction of $B(t \rightarrow Zq) < 3.7\%$ at 95% C.L. is obtained, which is currently the world's best limit on the anomalous vector coupling V_{tuZ} .

3.2 Searches for New Particles and Phenomena

3.2.1 Searches for High-Mass Particles

The CDF Collaboration performs a search for a heavy top-like object t' using 2.8 fb^{-1} of Tevatron Run II data [25]. A large t' branching ratio to Wq is assumed, as would be the case if $M_{t'} < M_{b'} + M_W$, a situation favoured by the constraint that an additional quark generation be consistent with precision electroweak data. The search is performed using two kinematic variables to separate the t' signal from the SM background: H_T , the sum of the transverse momenta of all objects in the event, and M_{reco} , the Wq reconstructed invariant mass. No evidence for t' is observed and an upper limit on $\sigma(t't')$ at 95% C.L. is set, excluding t' masses below 311 GeV, as shown in Figure 10 (left).

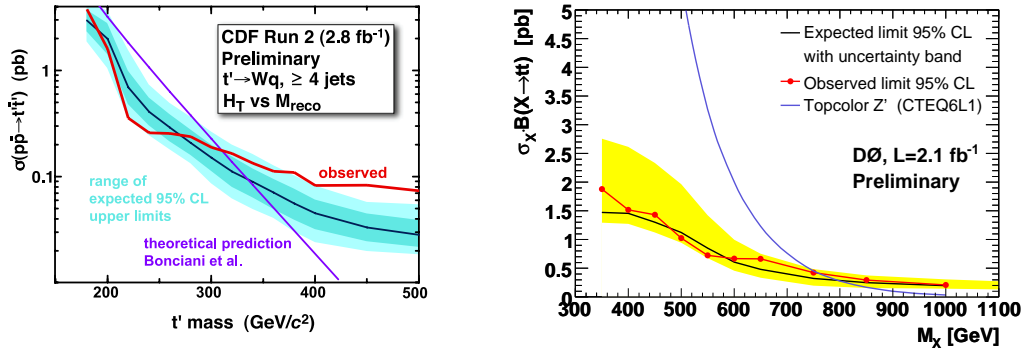


Figure 10: Left: Upper limit at 95% C.L. from CDF on the cross section for t' pair production at the Tevatron as a function of t' mass (red). The purple curve is the theoretical cross section. The blue band represents the range of limits expected from $\pm 1\sigma$ fluctuations in the predicted background (light blue corresponds to $\pm 2\sigma$). Right: Expected and observed 95% C.L. upper limits from DØ on $\sigma_X \cdot B(X \rightarrow t\bar{t})$ compared with the predicted top-colour-assisted technicolour cross-section for a Z' boson with a width of $\Gamma_{Z'} = 0.012 M_{Z'}$ as a function of the resonance mass M_X . The shaded band gives the range of expected limits corresponding to $\pm 1\sigma$ background fluctuations.

The DØ Collaboration performs a generic search for a narrow resonance decaying to top pairs $X \rightarrow t\bar{t}$, using 2.1 fb^{-1} of Tevatron Run II data [26]. The width Γ is assumed to be small compared to the detector mass resolution. The signal topology investigated is 3 or 4 jets plus a lepton, and missing transverse energy. No significant deviation from the SM expectation is observed in the reconstructed $M_{t\bar{t}}$ distribution. An upper limit on the production cross section $\sigma_X \cdot B(X \rightarrow t\bar{t})$ is derived as a function of resonance mass

M_X , as shown in Figure 10 (right). A model for Z' production is also shown, for which corresponding Z' masses $M_{Z'} < 760$ GeV are ruled out at 95% C.L.

Also performed by DØ and CDF are searches for heavy resonances decaying to fermion pairs in the di-jet, di-electron, four-electron, and electron plus missing transverse energy channels. No significant excess is observed in the data in all cases, and improved limits are set on the production of such particles, often extending well beyond 1 TeV, as is the case of the colour-octet techni- ρ (up to 1.1 TeV) and axigluon and flavour-universal colouron (up to 1.25 TeV) models [27].

3.2.2 Excited Fermion Searches

The existence of excited states of leptons and quarks is a natural consequence of models assuming composite fermions, and their discovery would provide convincing evidence of a new scale of matter. The production and decay of such particles is described in gauge-mediated (GM) and contact-interaction (CI) models.

DØ has searched for e^* in the process $p\bar{p} \rightarrow e^*e$, with subsequent e^* decay to an electron plus a photon [28]. Events with two isolated high P_T electrons and one isolated high P_T photon are selected in 1 fb^{-1} of data, where the SM background is dominated by the Drell-Yan process, $DY + \gamma \rightarrow e^+e^-\gamma$. No excess is seen in the data, and therefore 95% C.L. limits are derived, including both CI and GM decays. The resulting limits are shown as a function of m_{e^*} in Figure 11 (left), together with predictions of the CI model for different choices of the compositeness scale Λ . For $\Lambda = 1$ TeV, masses below 756 GeV are excluded. The excited

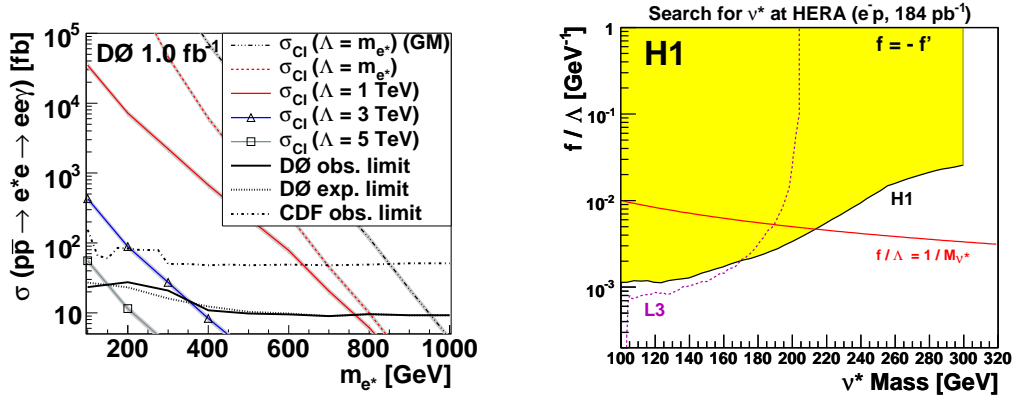


Figure 11: Left: The DØ measured and expected limits on cross section times branching fraction, compared to the CI model prediction for different choices of Λ . Also shown is the prediction under the assumption that no decays via contact interactions occur (GM). The observed limit from CDF is also indicated. Right: H1 exclusion limit at 95% C.L. on the coupling f/Λ as a function of the mass of the excited neutrino with the assumption $f = -f'$. The excluded domain, based on all H1 e^-p data, is represented by the shaded area. The dashed line corresponds to the exclusion limit obtained at LEP by L3.

electron decay channels $e^* \rightarrow e\gamma$, $e^* \rightarrow eZ$ and $e^* \rightarrow \nu W$ with subsequent hadronic or leptonic decays of the W and Z bosons are examined at HERA in a search for excited electrons by H1 [29]. In this search, which uses the complete H1 $e^\pm p$ data sample of 475 pb^{-1} integrated

luminosity, no indication of a signal is observed. New limits on the production cross section of excited electrons are obtained within a GM model, where an upper limit on the coupling f/Λ as a function of the excited electron mass is established for the specific relation $f = +f'$ between the couplings. Assuming $f = +f'$ and $f/\Lambda = 1/M_{e^*}$ excited electrons with a mass lower than 272 GeV are excluded at 95% C.L. For the first time in ep collisions, gauge and four-fermion contact interactions are also considered together for e^* production and decays, although it is found that the CI term improves the limit on $1/\Lambda$ only slightly, demonstrating that the GM mechanism is dominant for excited electron processes at HERA.

Using the full e^-p data sample collected by the H1 experiment at HERA with an integrated luminosity of 184 pb^{-1} a search for the production of excited neutrinos is performed [30]. Due to the helicity dependence of the weak interaction and given the valence quark composition and density distribution of the proton, the ν^* production cross section is predicted to be much larger for e^-p collisions than for e^+p . The excited neutrino decay channels $\nu^* \rightarrow \nu\gamma$, $\nu^* \rightarrow \nu Z$ and $\nu^* \rightarrow eW$ with subsequent hadronic or leptonic decays of the W and Z bosons are considered and no indication of a ν^* signal is found. Upper limits on the coupling f/Λ as a function of the excited neutrino mass are established for specific relations between the couplings. Assuming $f = -f'$ and $f/\Lambda = 1/M_{\nu^*}$, excited neutrinos with a mass lower than 213 GeV are excluded at 95% C.L., as shown in Figure 11 (right). The excluded region is greatly extended with respect to previous results and demonstrates the unique sensitivity of HERA to excited neutrinos with masses beyond the LEP reach.

3.2.3 Searches for Leptoquarks

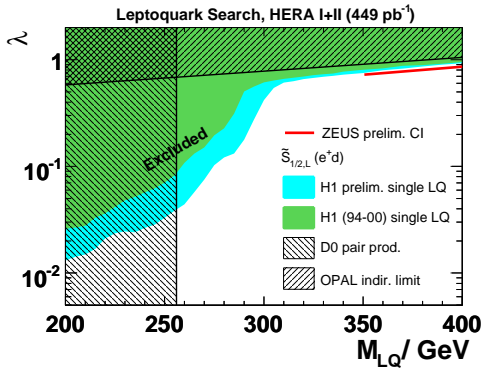


Figure 12: H1 exclusion limits at 95% C.L. on the coupling λ as a function of the LQ mass for the $\tilde{S}_{1/2,L}$ leptoquark in the framework of the BRW model. Corresponding limits from LEP (OPAL) and the Tevatron (DØ) are also shown, as well as the indirect CI limits from ZEUS (see section 3.2.4).

A search for leptoquark (LQ) production is performed by H1 at HERA in the 14 LQ framework of the Buchmüller, Rückl and Wyler (BRW) model, using the polarised e^\pm HERA II data [31]. LQs may be resonantly produced at HERA up to the centre-of-mass energy, beyond which the production mechanism is CI-like. An irreducible SM background is present from neutral and charged current DIS. No signal is observed in the DIS mass spectra and constraints on LQs are set, which extend beyond the domains previously excluded. For a coupling of electromagnetic strength, LQ masses below 291–330 GeV are ruled out at HERA, depending on the LQ type. In a separate search of the second-generation LQs at HERA, no signal for the lepton flavour violating (LFV) process $ep \rightarrow \mu X$ is found in the complete H1 e^- HERA II data set [32]. For Yukawa couplings of electromagnetic strength, LQs mediating the LFV process $e \rightarrow \mu$ are ruled out for LQ masses up to 433 GeV.

In $p\bar{p}$ collisions, LQs would be produced in pairs via the strong interaction. The production rate is thus essentially independent of the unknown Yukawa couplings. The most recent LQ

Final state	CDF			DØ		
	1 st gen.	2 nd gen.	3 rd gen.	1 st gen.	2 nd gen.	3 rd gen.
$\ell\ell jj$	236 GeV	225 GeV	151 GeV	256 GeV	251 GeV	180 GeV
$\ell\nu jj$	205 GeV	208 GeV	-	234 GeV	214 GeV	-
$\nu\nu jj$	177 GeV	177 GeV	167 GeV	136 GeV	136 GeV	229 GeV

Table 2: Summary of the 95% C.L. limits set by CDF and DØ on LQ masses of each generation, from searches using different final states containing 2, 1 or 0 charged leptons ℓ .

searches at the Tevatron have concentrated on $jj\nu\nu$ and $jj\mu\nu$ final states, more details of which can be found in [33]. Table 2 summarises all of the latest limits obtained by CDF and DØ for the different final states to which the different types of LQ could contribute. This table represents all the constraints for each of the three generations of LQs, imposed by the Tevatron on a generic LQ model.

3.2.4 Contact Interactions

New interactions between electrons and quarks at HERA involving mass scales above the centre-of-mass energy can modify the deep inelastic $e^\pm p$ scattering cross sections at high Q^2 via virtual effects, resulting in observable deviations from the SM predictions. Four-fermion contact interactions are an effective theory, which allows a general description of their effects. Various scenarios are considered by H1 [34] and ZEUS [35]. In the general case (also referred to as compositeness models), limits on the effective “new physics” mass scale Λ (the compositeness scale) are extracted assuming that the coefficients η of the various terms in the effective Lagrangian are given by $\eta = \pm 4\pi/\Lambda^2$. Figure 13 shows the results obtained by ZEUS for different compositeness models, based on the analysis of 1994–2006 data. Limits on the effective mass scale Λ range from 2–8 TeV.

For a model with large extra dimensions (LED), where cross section deviations are expected due to a graviton-exchange contribution, ZEUS set limits on the effective Planck mass scale M_S , and scales up to 0.90 TeV are excluded at 95% C.L. Direct searches for LED performed at the Tevatron in the form of graviton production also imply $\Lambda > 1.5$ TeV, with

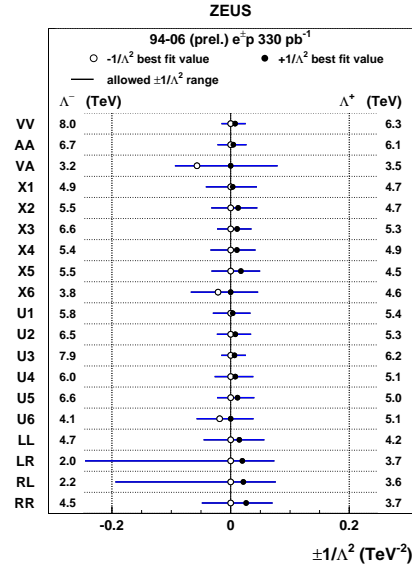


Figure 13: Results for general contact interaction models (compositeness models) obtained using the combined e^+p and e^-p data from ZEUS (1994–2006). Horizontal bars indicate the 95% C.L. limits on $\eta/4\pi = \epsilon/\Lambda^2$ and values outside these regions are excluded. Λ^\pm are the 95% C.L. limits on the compositeness scale for $\epsilon = \pm 1$.

$M_G > 1$ TeV [36]. Searches for possible quark substructure can be performed at HERA by measuring the spatial distribution of the quark charge. By using the *classical* form factor approximation, and assuming that both electron and exchanged bosons are point-like, limits on the mean-square radius of the electroweak charge of the quark are set, where quark radii bigger than $0.74 \cdot 10^{-16}$ cm (H1) and $0.62 \cdot 10^{-16}$ cm (ZEUS) are excluded at 95% C.L. Contact interactions can also be used to describe the effects of virtual LQ production or exchange at HERA, in the limit of large LQ mass $M_{LQ} \gg \sqrt{s}$. Indirect LQ limits from ZEUS [35] are shown in the CI kinematic domain in Figure 12, compared to the direct H1 exclusion limits discussed above.

3.3 Supersymmetry

In the search for new phenomena, a well-motivated extension to the SM is supersymmetry (SUSY), which relates particles with different spin. SUSY is one of the most promising ways to solve crucial problems of the SM. This spacetime symmetry links bosons to fermions and introduces supersymmetric partners (sparticles) to all SM particles.

3.3.1 SUSY Searches in the mSUGRA Model

Searches for squarks and gluinos are performed by the CDF and DØ Collaborations, using Tevatron Run II data [37]. The searches are performed in the minimal super gravity (mSUGRA) model with the lightest neutralino $\tilde{\chi}_1^0$ as the lightest supersymmetric particle (LSP). Three different regimes are defined, leading to the analysis of three separate final states: events with 2 jets, 3 jets and at least 4 jets, all in combination with missing transverse energy. All squark species are considered except the stop (CDF and DØ) and the sbottom (CDF). The main SM background is due to $W/Z +$ jets, di-bosons, and $t\bar{t}$ events. A good agreement is observed between data and the SM expectation in samples of 2 fb^{-1} . Lower limits are derived on the masses of squarks and gluinos, taking into account the systematic and statistical uncertainties. The limits from the DØ experiment are shown in Figure 14 (left), where for $\tan \beta = 3$, $A_0 = 0$, and $\mu < 0$, squark masses lower than 392 GeV and gluino masses lower than 327 GeV are excluded at 95% C.L. The CDF and DØ results are the best constraints to date on the squark and gluino masses.

One of the promising modes for SUSY detection at hadron colliders is that of chargino-neutralino associated production with decay into a trilepton signature. Charginos decay into a single lepton through a slepton or gauge boson, and neutralinos similarly decay to two detectable leptons. Thus the detector signature is three SM leptons with associated missing energy from the undetected neutrinos and lightest neutralinos, $\tilde{\chi}_1^0$, in the event. Due to its electroweak production, this is one of the few *jet-free* SUSY signatures. CDF performs a search using 2 fb^{-1} of data for a series of trilepton and dilepton + track exclusive channels [38]. Good agreement is observed between the data and the SM. As no clear signal is seen, upper limits on cross section times branching ratio are derived as a function of chargino mass, as shown in Figure 14 (right). A chargino lower mass limit of 145 GeV is obtained by CDF and in a similar analysis a lower mass limit of 145 GeV is also obtained by DØ.

As the turn-on of the LHC approaches, the discovery reach of ATLAS and CMS at the LHC in different search channels has been investigated using mSUGRA parameter scans [39]. Gluino and squark masses less than $\mathcal{O}(1)$ TeV are reported to be within reach after having

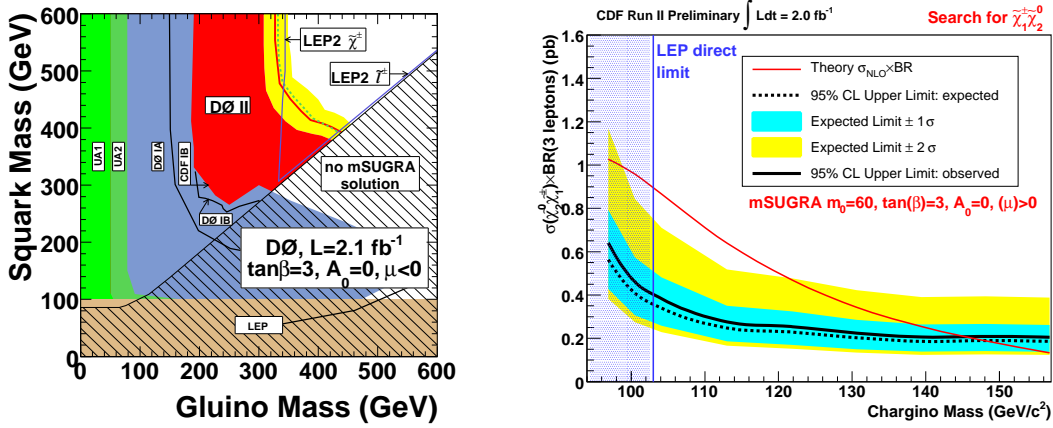


Figure 14: Left: Limits on squark and gluino masses from DØ. Right: CDF cross section times branching ratio upper limit as a function of chargino mass.

accumulated and understood an integrated luminosity of about 1 fb⁻¹.

3.3.2 SUSY Searches in the GMSB Model

In SUSY models with gauge mediated supersymmetry breaking (GMSB) the gravitino is the lightest SUSY particle (LSP), while the lightest neutralino or slepton is the next-to-lightest sparticle (NLSP). GMSB models offer a possibility to break SUSY at a low scale compared to that of generic mSUGRA models. At the Tevatron, cascade decays of pair-produced neutralinos to LSPs produce a final state featuring large missing transverse energy (from the gravitinos) and two photons (or leptons). The DØ experiment has searched for such a topology using 1 fb⁻¹ of data and, in the absence of a signal, set the current best limits on the masses of the neutralino $M_{\tilde{\chi}_1^0} > 125$ GeV, the chargino $M_{\tilde{\chi}_1^\pm} > 229$ GeV and the symmetry breaking scale $\Lambda > 91.5$ TeV [40].

In order to estimate the LHC discovery potential of the di-photon channel, a scan of the breaking scale Λ and $\tan\beta$ has been performed using a fast simulation. In this region the neutralino is usually the NLSP, except for large $\tan\beta$. Figure 15 shows the contour lines with 5 signal events for different integrated luminosities collected by the ATLAS experiment after prompt photon event selection [41]. In the regions below and left of the lines a discovery

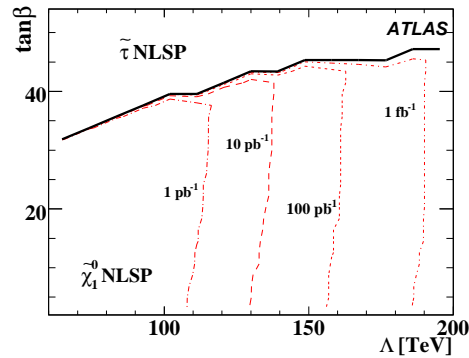


Figure 15: Contour lines with 5 di-photon + missing transverse energy signal events in the Λ - $\tan\beta$ plane for different integrated luminosities collected by the ATLAS experiment.

could be made with the corresponding amount of data assuming negligible background. In the high $\tan\beta$ region the $\tilde{\tau}$ is the NLSP and no photons occur in the decay chain. In general, it is found that the discovery potential extends to significant regions of the parameter space not excluded by the current limits, even with early LHC data. Similar studies have been performed for CMS with comparable results.

References

- [1] V. M. Abazov *et al.* (DØ Collaboration), Phys. Rev. Lett. **100** 241805 (2008).
- [2] A. Abulencia *et al.* (CDF Collaboration), Phys. Rev. Lett. **98** 161801 (2007);
D. Acosta *et al.* (CDF Collaboration), Phys. Rev. **D71** 091105 (2005).
- [3] T. Aaltonen *et al.* (CDF Collaboration), Phys. Rev. Lett. **100** 201801 (2008).
- [4] V. M. Abazov *et al.* (DØ Collaboration), arXiv:0808.0703 [hep-ex] (2008).
- [5] R. Wanke, arXiv:0807.2735 [hep-ex] (2008).
- [6] ZEUS Collaboration, contributed paper to *HEP-EPS 2007*, abstract **85**, ZEUS-prel-07-023.
- [7] CDF Collaboration, CDF Note 9431 (2008);
CDF Collaboration, CDF Note 9114 (2008).
- [8] V. M. Abazov *et al.* (DØ Collaboration), Phys. Rev. **D78** 012005 (2008).
- [9] ZEUS Collaboration, contributed paper to *ICHEP 2006*, ZEUS-prel-06-003.
- [10] H1 Collaboration, contributed paper to *HEP-EPS 2007*, abstract **230**, H1prelim-07-041.
- [11] K. McFarland, these proceedings and references therein.
- [12] CDF and DØ Collaborations, arXiv:0808.1089 [hep-ex] (2008).
- [13] V. M. Abazov *et al.* (DØ Collaboration), Phys. Rev. Lett. **100** 192004 (2008).
- [14] M. Cacciari *et al.*, arXiv:0804.2800 [hep-ph] (2008).
- [15] S. Moch and P. Uwer, arXiv:0804.1476 [hep-ph] (2008).
- [16] CDF and DØ Collaborations, arXiv:0808.0534 [hep-ex] (2008).
- [17] H1 Collaboration, contributed paper to *HEP-EPS 2007*, abstract **199**, H1prelim-07-061.
- [18] T. Aaltonen *et al.* (CDF Collaboration), Phys. Rev. **D78** 112002 (2008);
C. Henderson (for the CDF Collaboration), arXiv:0805.0742 [hep-ex] (2008).
- [19] F. D. Aaron *et al.* (H1 Collaboration), submitted to Phys. Lett. **B**, arXiv:0806.3987 [hep-ex] (2008);
ZEUS Collaboration, preliminary results ZEUS-prel-07-022, ZEUS-prel-08-006.
- [20] H1 and ZEUS Collaborations, contributed paper to *LP 2007*, H1prelim-07-166, ZEUS-prel-07-024.
- [21] S. Chekanov *et al.* (ZEUS Collaboration), arXiv:0807.0589 [hep-ex] (2008);
H1 Collaboration, contributed paper to *HEP-EPS 2007*, abstract **228**, H1prelim-07-063;
H1 Collaboration, contributed paper to *HEP-EPS 2007*, abstract **227**, H1prelim-07-064.
- [22] H1 and ZEUS Collaborations, contributed paper to *HEP-EPS 2007*, abstract **196**, H1prelim-07-162,
ZEUS-prel-07-029.
- [23] H1 Collaboration, contributed paper to *HEP-EPS 2007*, abstract **776**, H1prelim-07-163.
- [24] CDF Collaboration, submitted to Phys. Rev. Lett., arXiv:0805.2109 [hep-ex] (2008).
- [25] T. Aaltonen *et al.* (CDF Collaboration), Phys. Rev. Lett. **100** 161803 (2008);
CDF Collaboration, CDF Note 9446 (2008).
- [26] DØ Collaboration, DØ Note 5600-CONF (2008).
- [27] CDF Collaboration, CDF Note 9246 (2008).
- [28] V. M. Abazov *et al.* (DØ Collaboration), Phys. Rev. **D77** 091102(R) (2008).
- [29] F. D. Aaron *et al.* (H1 Collaboration), submitted to Phys. Lett. **B**, arXiv:0805.4530 [hep-ex] (2008).
- [30] F. D. Aaron *et al.* (H1 Collaboration), Phys. Lett. **B663** 382 (2008).

- [31] H1 Collaboration, preliminary results, H1prelim-07-164.
- [32] H1 Collaboration, preliminary results, H1prelim-07-167.
- [33] P. Beauchemin, these proceedings and references therein.
- [34] H1 Collaboration, contributed paper to *LP 2007*, H1prelim-07-141.
- [35] ZEUS Collaboration, contributed paper to *ICHEP 2006*, ZEUS-prel-06-018.
- [36] CDF Collaboration, submitted to Phys. Rev. Lett., arXiv:0807.3132 [hep-ex] (2008).
- [37] V. M. Abazov *et al.* (DØ Collaboration), Phys. Lett. **B660** 449 (2008);
CDF Collaboration, CDF Note 9229 (2008).
- [38] CDF Collaboration, submitted to Phys. Rev. Lett., arXiv:0808.2446 [hep-ex] (2008);
DØ Collaboration, DØ Note 5464-CONF (2007).
- [39] R. Brunelière, these proceedings and references therein.
- [40] V. M. Abazov *et al.* (DØ Collaboration), Phys. Lett. **B659** 856 (2008).
- [41] ATLAS Collaboration, ATLAS Note SUSY CSC 8, to be published.